Anomalous diffusion of proteins in sheared lipid membranes

Atefeh Khoshnood[1,2] and Mir Abbas Jalali[1,*]

[1]*Computational Mechanics Laboratory, Department of Mechanical Engineering, Sharif University of Technology, Azadi Avenue, Tehran, Iran*

[2]*Center of Excellence in Design, Robotics and Automation, Department of Mechanical Engineering, Sharif University of Technology, Azadi Avenue, Tehran, Iran*

(Received 4 November 2012; revised manuscript received 8 August 2013; published 5 September 2013)

We use coarse grained molecular dynamics simulations to investigate diffusion properties of sheared lipid membranes with embedded transmembrane proteins. In membranes without proteins, we find normal in-plane diffusion of lipids in all flow conditions. Protein embedded membranes behave quite differently: by imposing a simple shear flow and sliding the monolayers of the membrane over each other, the motion of protein clusters becomes strongly superdiffusive in the shear direction. In such a circumstance, the subdiffusion regime is predominant perpendicular to the flow. We show that superdiffusion is a result of accelerated chaotic motions of protein-lipid complexes within the membrane voids, which are generated by hydrophobic mismatch or the transport of lipids by proteins.

DOI: 10.1103/PhysRevE.88.032705 PACS number(s): 87.15.Vv, 87.16.dj, 87.14.ep, 82.20.Wt

I. INTRODUCTION

Lipid bilayers are the essential parts of any living cell. They constitute the main body of the cell membrane while being found in different organelles inside the cell. The cell membrane hosts collections of proteins and lipid rafts, and it is crowded with a variety of biomolecules. In such nonhomogeneous and diverse environments, the diffusion of protein molecules in lipid bilayers plays a vital role in different biological processes like cell signaling. The diffusion of lipids and proteins is not a distinct phenomenon and depends on the environment and neighboring molecules [1] and even changes from cell to cell [2]. Transmembrane proteins diffuse as dynamic complexes with lipids [3,4], and their interactions with lipid molecules mediates traffic in cell membranes. Experiments show that the hydrophobic mismatch between proteins and lipids controls the diffusion coefficient of molecules inside a bilayer [5,6].

Anomalous sub- and superdiffusion processes are more efficient scenarios for finding a nearby target than normal diffusion [7,8], and they enhance the formation of protein complexes and signal propagation. According to experiments, the mean square displacement (MSD) of membrane channel proteins of the human kidney cell exhibits subdiffusion [9]. The addition of cholesterols to lipid membranes [10] and the augmented area coverage of membrane proteins [11] also lead to subdiffusion of lipids and proteins. Superdiffusivity has been observed in several physical systems and is often associated with Lévy flights. Prominent examples are the chaotic motion of particles in a rotating laminar flow [12] with long-range flights and horizontally vibrated grains which exhibit Lévy flight with small jumps compared to their diameter [13]. Nevertheless, an active component such as molecular motor can also be the source of superdiffusivity. A recent study by Köhler *et al.* [14] shows that in a gel composed of actin filaments, fascin molecules, and myosin-II filaments, the diffusion of small actin and fascin clusters is superdiffusive because of the work done by molecular motors.

In many conditions membranes are under shear. When a red blood cell (RBC) migrates through vessels smaller in diameter than itself, the RBC membrane is under shear. The blood flow exerts tangential shear stresses on vascular endothelia and initiates cellular processes like activating G protein-coupled receptors. These receptors are able to sense the fluid shear stress as an increase in the lateral membrane tension and subsequently go through conformational changes [15]. The temporal and spatial changes in the membrane fluidity, in response to shear flow, have been observed experimentally [16,17].

In this study we are interested in the diffusivity of lipid and protein molecules in flat membranes under shear flow and attempt to answer three fundamental questions using molecular dynamics (MD) simulations: (i) Do lipid molecules have different diffusion coefficients parallel and perpendicular to the flow direction? (ii) How does a simple shear flow influence the random motions of transmembrane proteins? (iii) Is there any correlation between the population of proteins and their diffusion in the membrane?

II. MODEL AND METHODS

We simulate lipid membranes utilizing a flexible lipid model [18] and triple-strand rigid proteins [19] [Fig. 1(a)]. Although different coarse grained models have been developed over the years [20], the model adopted here has the ability to mimic the physical properties of lipid membranes. The model is not a true coarse grained model but can qualitatively describe phenomena related to lipid membranes and associated transmembrane proteins as we will compare some of our results with true coarse grain and atomistic models. Our goal is to explore the effect of shear flow on the motion of lipid and protein molecules over nanosecond time scales. We perform MD simulations of an NVT ensemble, where the number of particles N, the volume V, and the temperature T are held constant. The Lees-Edwards boundary condition is employed to generate simple shear flow with the shear rate $\dot{\gamma}$ [21]. Other boundary conditions are periodic. The temperature is set to 324 K so that the system is safely above the gel to liquid phase transition temperature of different phosphatidylcholine lipid

*mjalali@sharif.edu

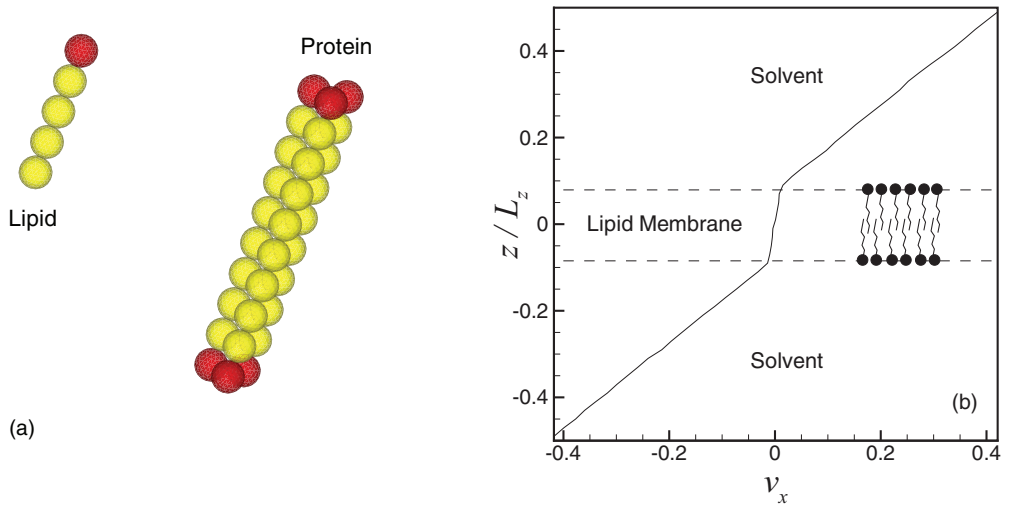

FIG. 1. (Color online) (a) The models of lipid and protein molecules. Red (dark gray) and yellow (light gray) spheres are hydrophilic and hydrophobic particles, respectively. (b) Velocity profile of a sample solvent-membrane system under simple shear flow with $\dot{\gamma} = 0.03\tau^{-1}$. The dashed lines mark the average boundaries of the solvent columns and the membrane.

bilayers. A detailed description of the model can be found in Khoshnood *et al*. [19].

We express the position and velocity vectors of particles in the Cartesian (x,y,z) coordinate system whose origin is located at the center of our cubic simulation box. The x and y axes lie in the membrane plane, and the z axis is perpendicular to that. MD scales of length, time, mass, and energy are $\sigma = 1/3$ nm, $\tau = 1.4$ ps, $N_{\text{avo}}\, m = 36$ g/mol, and $N_{\text{avo}}\, \epsilon = 2$ kJ/mol, respectively. N_{avo} is Avogadro's number. In all simulations, the dimensions of the box along the coordinates axes, L_x, L_y and L_z, are set to $L_x = L_y = L_z = 28.71\sigma$. The total number of particles equals $N = 15\,625$, which gives a fixed number density, $\rho = 2/(3\sigma^3)$, and a constant average fluid pressure of $(1.7 \pm 0.1)\epsilon\sigma^{-3}$ for all simulations. Here, we note that isotropic pressure control is not appropriate in the simulation of lipid membranes since their volume is constant in the laboratory and biological conditions. However, a fixed number density will give a constant average pressure, and physical properties of lipid membranes with different number of lipids and proteins can be compared. Physical quantities are measured using a run time of $\approx 5000\tau$. An important mechanical property of every membrane is the surface tension ζ, which mainly affects the diffusion of lipid molecules. We compute the tension of our model membranes from

$$\zeta = [P_{zz} - (P_{xx} + P_{yy})/2]L_z, \tag{1}$$

where $P_{\alpha\alpha}$ $(\alpha \equiv x,y,z)$ are the components of the pressure tensor [21].

In this study we apply MSD to determine the diffusion properties of randomly moving particles. The diffusion coefficient is thus calculated using the Einstein expression

$$D_{\alpha\alpha} = \lim_{t\to\infty} \frac{1}{2Nt} \left\langle \sum_{i=1}^{N} [q_{i\alpha}(t) - q_{i\alpha}(0)]^2 \right\rangle, \tag{2}$$

where $\alpha \in \{x,y,z\}$ and $q_{i\alpha}$ is the displacement due to the random motion of the ith particle in the α direction. The summation in Eq. (2) is taken over the particles of the same type. From here on, we will drop the summation sign for brevity. The operator $\langle \cdots \rangle$ denotes the canonical average. Equation (2) describes the regular Brownian motion when the MSD is linearly proportional to t. The diffusion process is anomalous should the MSD deviate from the linear form and obeys the relation

$$\langle [q_\alpha(t) - q_\alpha(0)]^2 \rangle = 2D^a_{\alpha\alpha} t^a, \tag{3}$$

where a is the diffusion exponent and $D^a_{\alpha\alpha}$ is the fractional diffusion coefficient. The regimes with $0 < a < 1$ and $a > 1$ are subdiffusive and superdiffusive, respectively. To obtain smooth MSD curves, we evolve systems of 80 different initial conditions and report their ensemble-averaged diffusion coefficients and MSDs. The diffusion of lipids is investigated by tracing the motion of their head groups. Proteins are traced using their centers of mass.

In equilibrium models without external shearing, there is no streaming in the solvent-membrane system. Therefore, the flux of particles is associated with their random motions, and any displacement is due to thermal fluctuations. In sheared membranes, however, there is a combination of streaming and diffusive fluxes. We thus need to distinguish and eliminate the streaming flux when calculating the MSD. Let us define the actual velocity components of the jth particle as $v_{j\alpha} = \langle v_\alpha \rangle + \tilde{v}_{j\alpha}$, where $\langle v_\alpha \rangle$ is the average streaming velocity and $\tilde{v}_{j\alpha}$ is the peculiar velocity whose time integral gives the displacements in Eqs. (2) and (3). In equilibrium models, the average velocities $\langle v_\alpha \rangle$ vanish, and we obtain $q_{j\alpha} = \int v_{j\alpha} dt = \int \tilde{v}_{j\alpha} dt$. With external shearing, the flow is always imposed in the x direction. Therefore, $v_{jy} = \tilde{v}_{jy}$ and $v_{jz} = \tilde{v}_{jz}$ are directly integrated to find the corresponding displacements. When the simulation box is uniformly filled with one type of particles (let us say solvent particles), one readily finds $\tilde{v}_{jx} = v_{jx} - z\dot{\gamma}$. In the presence of a lipid bilayer, the vertical velocity profile in the z direction is no longer linear [see Fig. 1(b)]. Therefore, to obtain the MSD of lipids, we define $\langle v_x \rangle$ as the average velocity of the layer where the head groups of phospholipids reside and obtain $q_{jx} = \int (v_{jx} - \langle v_x \rangle) dt$. It

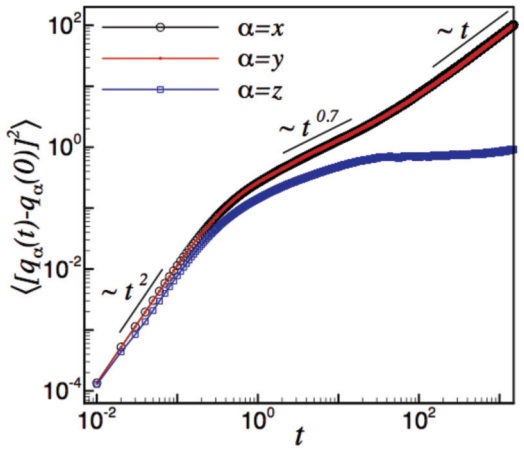

FIG. 2. (Color online) MSD of lipid molecules for the membrane with 600 lipids and for $\Delta t = 0.01\tau$. The membrane is under simple shear flow with $\dot{\gamma} = 0.03\tau^{-1}$, and each lipid molecule has been hydrated by almost 20 solvent particles. The coordinate axes are in logarithmic scale.

is remarked that transmembrane proteins do not experience streaming movements, $\langle v_\alpha \rangle = 0$, because the shear forces exerted on their end points from the upper and lower solvent columns are equal and in opposite directions.

III. DIFFUSION OF LIPIDS

The lateral diffusion of lipids under equilibrium conditions is enhanced as the membrane tension increases. This has been observed in simulations by atomistic [22] and coarse grained models [23] and is because, by stretching the membrane, the area per lipid increases and more space is provided for the free motion of lipids. Our simulations with this very simple model show the same pattern. By turning on the shear flow, lipid molecules undergo an initial ballistic motion that transforms into an interval of subdiffusion with $a = 0.7$ (Fig. 2). The transient anomalous state has been observed in atomistic simulations [24] as well. After the transient anomalous diffusion and over longer time scales a normal diffusion with $a = 1$ is observed (Fig. 2). It is noted that we have found similar MSD profiles for lipid molecules in equilibrium and sheared systems, and in both cases lipids ultimately develop normal diffusion. Although Kneller *et al*. [25] reported a permanent subdiffusive behavior by the atomistic simulation of lipid membranes in equilibrium, experiments support a final regular diffusion regime, as we do, even in the presence of obstacles [26]. We conclude that the diffusion regime of lipid molecules is invariant with and without external shearing.

The diffusion coefficients obtained from the normal diffusion region of MSD plots are larger for smaller shear rates. For example, for a membrane of $N_l = 600$ lipid molecules, we find $\zeta = (1.4846 \pm 0.2624)\epsilon/\sigma^2$, $D_{xx} = 0.0338\sigma^2/\tau$, and $D_{yy} = 0.0334\sigma^2/\tau$. For the same system under a shear flow of $\dot{\gamma} = 0.03\tau^{-1}$, the membrane tension drops to $\zeta = (0.8163 \pm 0.2727)\epsilon/\sigma^2$, and the diffusion coefficients reduce to $D_{xx} = 0.0318\sigma^2/\tau$ and $D_{yy} = 0.0332\sigma^2/\tau$. The reason is that the membrane thickness increases for higher shear rates and the tension decreases without any change in the area per lipid [19]. Consequently, the fluidity of the membrane decreases and slows down the diffusion process. After applying the shear force, we find that D_{xx} drops by about 6%, while D_{yy} remains almost constant with only 0.4% change, which is not statistically significant since it is less than the mean standard error for diffusion coefficients, which is less than 1%. The difference between D_{xx} and D_{yy} is indistinguishable in Fig. 2. We speculate that the alignment of lipid chains with the flow breaks the isotropy and yields $D_{xx} \neq D_{yy}$. Atomistic simulation of the lipid membrane [22] has shown that increasing the tension of the membrane, induced by altering the area per lipid, results in larger lateral diffusion coefficients. This change is not linear with tension, and Muddana *et al*. [22] have reported a 4%–28% increase in the lateral diffusion coefficient. Coarse grained simulations [23] showed that for larger tensions the increase in diffusion coefficient slows down and depends on the range of tension. In our simulation, shear flow induces a 45% change in tension and, consequently, results in a different diffusion coefficient in the flow direction. In the z direction, perpendicular to the membrane plane, our MSD plots always show a confined motion, as is expected.

IV. DIFFUSION OF PROTEINS

We add rod-like proteins to the membrane and simulate models with different protein concentrations that vary significantly from cell to cell. Since proteins increase the membrane tension as they perturb the distribution of lipids [19], we increase the number of lipids (proportional to proteins) to keep the membrane almost tensionless. In equilibrium and for a membrane with a single embedded protein with $\zeta = (0.1153 \pm 0.1742)\epsilon/\sigma^2$, we can measure the diffusion coefficients $D_{\alpha\alpha}$ since the MSD of protein shows an ultimate regular diffusion. We find $D_{xx} = 0.0253\sigma^2/\tau$ and $D_{yy} = 0.0254\sigma^2/\tau$, which are equivalent to $D_{xx} \approx D_{yy} \approx 2 \times 10^{-9}\mathrm{m}^2/\mathrm{s}$ with less than 1% error. These values are larger than experimental values by two orders of magnitude. The obvious reason is the effect of coarse graining that has reduced the interdigitation and friction between molecules and allows for faster movements of particles. The reduced friction affects both the membrane component and solvent motion and, consequently, decreases both solvent and membrane viscosity. Viscosity of a fluid is a determinant of mobility or diffusion in that medium. Another minor source of discrepancy is the smaller size of our model proteins compared to real integral proteins.

We note that the average diffusive behavior of lipids is unaffected by the presence of proteins. We computed the average MSD profile of lipids for the above system and found the same pattern of initial ballistic regime, transient subdiffusive region, and final normal diffusion. The diffusion coefficients for our model proteins are smaller than model lipid molecules by a factor of 0.75. This is expected because of the larger size and mass of proteins compared to lipids.

The same initial ballistic motion as observed for lipids is recovered for proteins by using a time step as small as $\Delta t = 0.0005\tau$ for $t < 0.01\tau$. This regime is shared by all the systems regardless of the shear rate and the number of proteins. By putting the system under simple shear flow, proteins undergo

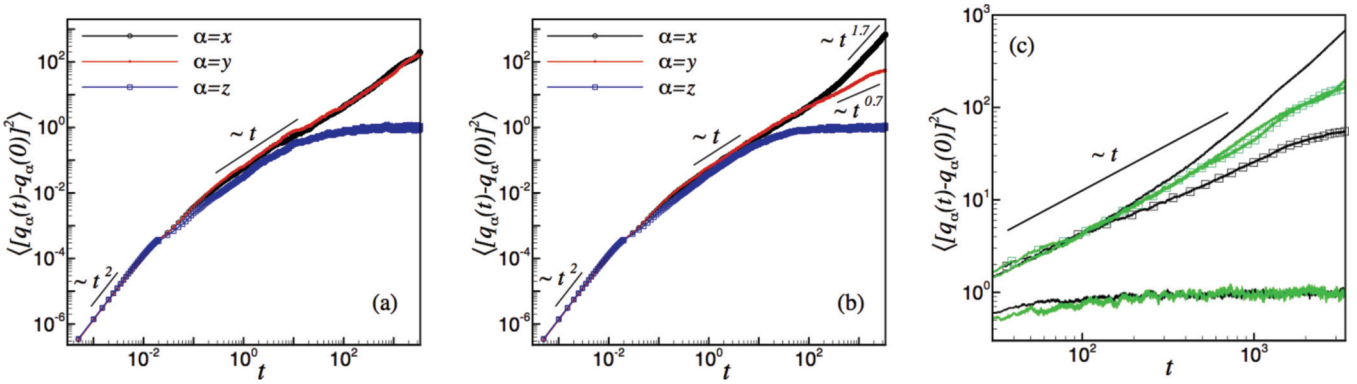

FIG. 3. (Color online) MSD of protein molecules in a protein-embedded model with (a) 2 and (b) 4 proteins, which corresponds to 640 and 660 lipids, respectively. We have used $\Delta t = 0.0005\tau$ up to $t = 0.02\tau$ and $\Delta t = 0.01\tau$ for $t > 0.02\tau$. In both (a) and (b) the membrane is under simple shear flow with $\dot{\gamma} = 0.03\tau^{-1}$, and each lipid molecule has been hydrated by almost 20 solvent particles. The coordinate axes are in logarithmic scale. (c) Close-up of the upper parts of the MSD profiles, with the green (light gray) and black lines corresponding to the systems in (a) and (b), respectively. The profiles with square symbols correspond to the y direction.

Brownian motion when only two proteins are used [Fig. 3(a)]. One could anticipate this result, for single proteins cannot remarkably perturb the distribution of lipids and change the diffusion properties of the membrane.

However, we observe that four proteins form two double-protein clusters (due to the depletion force) and exhibit a strong superdiffusive motion parallel to the flow. Figure 3(b) shows how after $t \sim 100\tau$ the normal diffusion regime transforms to strong superdiffusion with $a = 1.7$ in the x direction. Interestingly, this exponent is the same as the superdiffusion exponent found by Köhler *et al.* [14] for active diffusion of protein clusters by molecular motors. Because of the crowding effect and an increase in the concentration of proteins [1], our results show a subdiffusive behavior along the y axis with $a = 0.7$. Weigel *et al.* [9] observed $a = 0.8 \pm 0.1$ in experiments with channel proteins of a human kidney cell, and Javanainen *et al.* [27] found $a = 0.75 \pm 0.15$ by molecular simulations of aggregating NaK channel proteins. For clarity, the upper parts of the MSD profiles in Figs. 3(a) and 3(b) are plotted together in Fig. 3(c).

To rule out the effect of statistical errors in the development of anomalous behavior, we have divided the MSD profiles of the system with four proteins into smaller intervals and separately calculated a and its error over each interval using the curve fitting toolbox of MATLAB. We then assigned the mean value to the center of the time interval and plotted the calculated diffusion exponent versus time in Fig. 4. For instance, over the initial ballistic zone, we have obtained $a = 1.989 \pm 0.006$ from $t = 0.005\tau$ to $t = 0.01\tau$ and assigned this value to $t = 0.0075\tau$. Figure 4 shows that a approaches 1.7 and 0.7 in the x and y directions, respectively.

To understand the physical mechanism behind the observed anomaly, we conduct the following analysis. Let us define the local concentration of the head particles of lipid and protein molecules at the position $\boldsymbol{r}$ and time t as $f = \frac{1}{N_h}\sum_{i=1}^{N_h}[H(\delta_i) - H(\delta_i - \Delta)]$, where $\delta_i(t) = |\boldsymbol{r}_i(t) - \boldsymbol{r}|$ and $\boldsymbol{r}_i(t)$ is the position vector of the ith head particle. N_h denotes the total number of head particles in the monolayer, $H(\xi)$ is the Heaviside step function, and 2Δ is the typical size of the cross section of a protein cluster (or a protein-lipid complex). Our numerical experiments show $\Delta = 4\sigma$ is the best choice. We examine the trajectories of protein molecules and the spatial variation of the normalized distribution $\hat{f}(\boldsymbol{r},\Delta,t) = (f - f_{\min})/(f_{\max} - f_{\min})$ to explain the physics of observed superdiffusion. Here $f_{\min}$ and $f_{\max}$ are the minimum and maximum values of f at a given time t. Figure 5 demonstrates contour plots of $\hat{f}$ for the upper and lower monolayers at a randomly chosen time.

Figure 6(a) demonstrates the trajectories of a single protein molecule and two double-protein clusters in equilibrium and sheared systems, respectively. The equilibrium trajectory corresponds to regular diffusion because it covers a definite area. In the sheared system the trajectories are elongated and aligned with the flow direction, indicating a fractional random walk: local isotropic wanderings followed by small-step jumps mainly in the flow direction. These successive jumps can be interpreted by inspecting the contour plots of $\hat{f}(\boldsymbol{r},\Delta,t)$ over a long duration of time. The hydrophobic mismatch

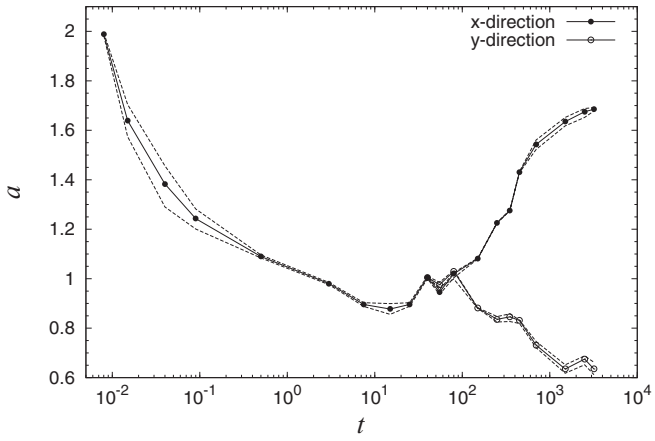

FIG. 4. The variation of the diffusion exponent a for the system in Fig. 3(b). Solid lines correspond to the mean values, and dashed lines show the error. For the y direction, a has been plotted only for $t > 30\tau$ because for $t < 30\tau$ the diffusion exponents of the x and y directions are almost identical. The horizontal coordinate axis is in logarithmic scale.

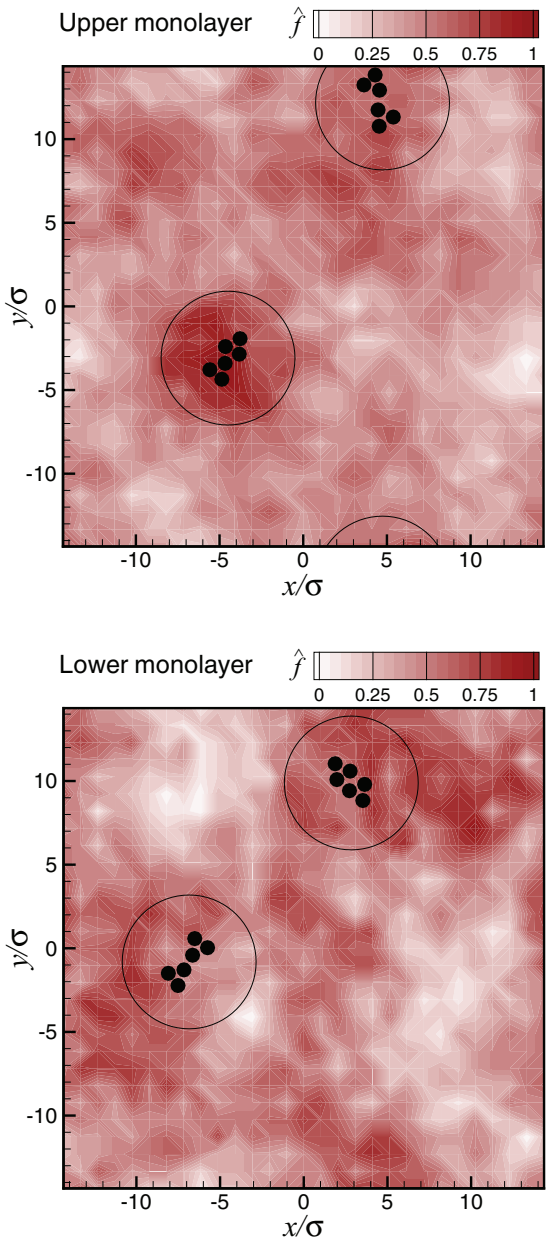

FIG. 5. (Color online) The local concentration $\hat{f}(\boldsymbol{r},\Delta,t)$ of head groups in the (top) upper and (bottom) lower leaflets of a sheared membrane at a randomly selected time for $\Delta = 4\sigma$. The head particles of proteins are shown by solid circles. Drawn circles have radii of Δ, and their centers lie at the centroid of the head particles of proteins. The flow with the shear rate $\dot{\gamma} = 0.03\tau^{-1}$ is in the x^+ and x^- directions for the upper and lower leaflets, respectively [cf. Fig. 1(b)]. The model has 660 lipids and 2 double-protein clusters. Since proteins are longer than the bilayer thickness, they are aligned in the shear flow, and their upper and lower head particles do not have the same coordinates.

between protein clusters (which have asymmetric big cross sections) and the membrane disturbs the bilayer thickness and the arrangement of nearby lipids. Moreover, proteins are able to transport their neighboring lipids with them and behave as dynamic complexes [3,4]. These two effects collaborate to create transient voids whose distribution can be described by $\hat{g} = 1 - \hat{f}$ (light shades in Fig. 5). When the bilayer is sheared, protein-lipid groups are pushed into the voids created by themselves or other groups or complexes and experience accelerated, and therefore superdiffusive, movements. It should be noted that during our simulations, the center of mass of the membrane and embedded proteins remains almost at the center of the coordinate system.

None of our samples show long-step straight motions of protein clusters. What we have seen are small-step jumps, which are comparable to the mean distance between protein clusters and voids [compare Figs. 5 and 6(a)]. We have computed the probability distribution function (PDF) of protein displacements and plotted it in Fig. 6(b). A Gaussian function has been fitted to the data by setting its maximum to the maximum of PDF, and its variance is found using the full width at half minimum of the PDF. The PDF exhibits a deviation from normal distribution and it has tails. We have also applied the Kolmogorov-Smirnov test [28] to confirm that the PDF is not a normal Gaussian. This is a clear indication of anomalous diffusion.

As we noted before, the ends of proteins are pulled in opposite directions by the two sheared solvent columns. An important question is why do protein clusters prefer to jump into the voids when the membrane is sheared? We have a simple explanation for this behavior: Two ends of proteins attract lipids from two different layers of the membrane. Thus, the symmetry in the distribution of the upper and lower protein-bound lipids is likely to break. Moreover, the shear force is exerted by the solvent on both the lipid and protein heads. The mentioned symmetry breaking thus leads to different force components at the upper and lower ends of protein-lipid complexes, and they will jump into a void in the direction specified by the broken symmetry. To quantify this process, we take a sample two-protein cluster and define $\boldsymbol{r}_u$ and $\boldsymbol{r}_l$ as the centers of mass of its protein heads in the upper and lower leaflets, respectively. We then compute

$$\xi(t_i) = \hat{f}(\boldsymbol{r}_u,\Delta,t_i) - \hat{f}(\boldsymbol{r}_l,\Delta,t_i), \tag{4}$$

which is proportional to the net shear force exerted on the cluster at the time step t_i: the local effective area in contact with a solvent column is determined by the number of head particles, and the shear force is calculated by multiplying the effective contact area by the shear rate and viscosity. $\xi(t_i)$ will be zero if the concentrations of the head particles of lipids are identical around the two heads of the cluster. Defining $\bar{\xi}$ as the average of $\xi(t_i)$, the autocorrelation function

$$A(t_{\rm lag}) = \frac{\sum_i [\xi(t_i + t_{\rm lag}) - \bar{\xi}][\xi(t_i) - \bar{\xi}]}{\sum_i [\xi(t_i) - \bar{\xi}]^2}, \tag{5}$$

plotted in Fig. 6(c) carries interesting information about the shear force experienced by the cluster: the correlation time $t_c \approx 23\tau$ shows a sustained accelerated motion of the cluster over $t_0 < t \lesssim t_0 + t_c$, independent of the initial time t_0. Moreover, the oscillatory decaying profile of $A(t_{\rm lag})$ shows a random symmetry breaking in the sense of deterministic chaos ([29], Sec. 5.3.4). The existence of a correlation time can also be verified by studying the cross-correlation function

$$C(t_{\rm lag}) = \int dt \int d\boldsymbol{r}\, \hat{f}(\boldsymbol{r},\Delta,t + t_{\rm lag})\hat{g}(\boldsymbol{r},\Delta,t) \tag{6}$$

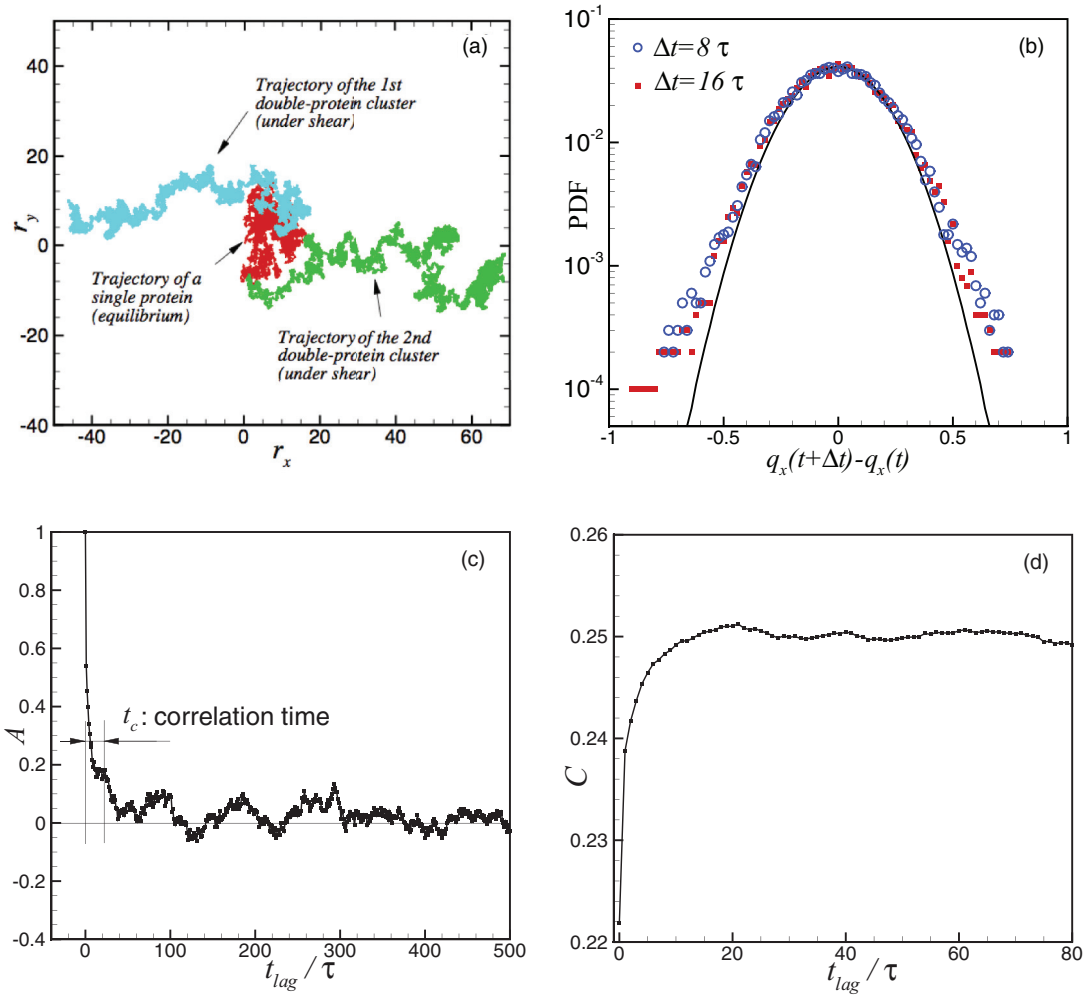

FIG. 6. (Color online) (a) Trajectories of a single protein in equilibrium and two double-protein clusters under shear flow as indicated by arrows. (b) PDF for the displacements of a sample two-protein cluster. The solid line shows the best Gaussian function fitted to the data. (c) Autocorrelation function $A(t_{\rm lag})$ for the difference between the head particle populations near the two ends of a protein cluster. The correlation time $t_c \approx 23\tau$ is defined at the point where $A(t_{\rm lag})$ abruptly drops below 10% of its maximum. We have taken 1000 successive samples in the time domain, with increments of 1τ, to compute A. (d) Cross-correlation function $C(t_{\rm lag})$ between the distribution of protein-lipid complexes and their neighboring voids. The integrals in C have been taken using a grid of 29×29 in the xy plane and 1000 successive points, with steps of 1τ, in the time domain.

over one of the leaflets. Figure 4(d) shows that $C(t_{\rm lag})$ of the upper leaflet steeply rises from $t_{\rm lag} = 0$ and peaks at $t_{\rm lag} \approx 21\tau$, which is the earliest time span that protein-lipid complexes need to occupy their nearest voids. This is quite consistent with the acceleration time scale of protein clusters predicted by the autocorrelation function $A(t_{\rm lag})$. For $t_{\rm lag} \gtrsim 21\tau$ the cross-correlation function remains almost flat because the size of a void is always bigger than the distance that a protein cluster travels during $t \sim O(t_c)$.

V. CONCLUSIONS

In this work, we use a toy model of proteins and lipids to simulate the dynamics of cell membranes undergoing shear flow. We calculate the MSD profile of lipids and proteins in equilibrium and a sheared system and compare our result with existing works in the literature. This simple model beautifully captures the basic regimes in the diffusive behavior of lipid molecules: the short initial ballistic regime, transient subdiffusive regime, and final normal diffusion. All-atom MD simulations show the same diffusive regions in the MSD profile of a lipid molecule [24]. Moreover, we show that shear flow reduces the tension of the membrane and consequently decreases the diffusion coefficient in the direction of flow. The fact that reducing membrane tension slows down lipid movement has been reported as the result of all-atom MD simulations [22] and experimental measurements [16].

Since there were a small number of protein molecules in the system, we did extensive MD simulations to obtain the final MSD profiles for proteins. Our C++ code, which has already been calibrated [19] for membranes under simple shear flow, is not parallel and allows only for small-scale simulations. We have recovered our results by LAMMPS for models in equilibrium conditions. However, LAMMPS does not have the capability of imposing simple shear flow conditions, and we could not use it to run our sheared systems over

longer time scales. Despite these limitations, the smooth MSD profiles obtained from our numerous samples clearly show the distinction between the regular diffusion of single proteins and anomalous diffusion of protein clusters. We explain this anomaly by deliberately examining the distribution of head particles of lipids and proteins and introducing a void generation mechanism. Our simulations cover time scales of the order of nanoseconds.

Cell responses to stimuli are fast due to the enhanced mobility of protein receptors. Considering our findings, superdiffusion of proteins under shear flow can play a dominant role in the process of signaling in endothelium cells, RBCs, liposomes used for targeted drug delivery, and other sheared membranes. We note that since the length and shape of proteins and their ability to attract neighboring lipids control the sizes of voids (there was no other mechanism in our models for void generation), the superdiffusion properties reported in this study are not universal and they highly correlate with the properties of embedded proteins. Simulations using detailed structures of lipids and proteins are needed to better assess the superdiffusive behavior in realistic cell membranes. Experimental exploration of our results can be done using single particle tracking [30], which can give the MSD of proteins directly.

ACKNOWLEDGMENTS

We thank the anonymous referees for their insightful comments that helped us improve the presentation of our results. A.K. was partially supported by the National Elites Foundation of Iran. We express our sincere thanks to Professor Ali Meghdari for his helpful discussions and encouragement.

[1] J. A. Dix and A. S. Verkman, Annu. Rev. Biophys. **37**, 247 (2008).
[2] S. Wieser, J. Weghuber, M. Sams, H. Stockinger, and G. J. Schuetz, Soft Matter **5**, 3287 (2009).
[3] P. S. Niemelä, M. S. Miettinen, L. Monticelli, H. Hammaren, P. Bjelkmar, T. Murtola, E. Lindahl, and I. Vattulainen, J. Am. Chem. Soc. **132**, 7574 (2010).
[4] A. Prasad, J. Kondev, and H. A. Stone, Phys. Fluids **19**, 113103 (2007).
[5] S. Ramadurai, A. Holt, L. V. Schafer, V. V. Krasnikov, D. T. S. Rijkers, S. J. Marrink, J. A. Killian, and B. Poolman, Biophys. J. **99**, 1447 (2010).
[6] Y. Gambin, M. Reffay, E. Sierecki, F. Homble, R. S. Hodges, N. S. Gov, N. Taulier, and W. Urbach, J. Phys. Chem. B **114**, 3559 (2010).
[7] G. Guigas and M. Weiss, Biophys. J. **94**, 90 (2008).
[8] F. Bartumeus, J. Catalan, U. L. Fulco, M. L. Lyra, and G. M. Viswanathan, Phys. Rev. Lett. **88**, 097901 (2002).
[9] A. V. Weigel, B. Simon, M. M. Tamkun, and D. Krapf, Proc. Natl. Acad. Sci. USA **108**, 6438 (2011).
[10] J. H. Jeon, H. Martinez-Seara Monne, M. Javanainen, and R. Metzler, Phys. Rev. Lett. **109**, 188103 (2012).
[11] S. Ramadurai, A. Holt, V. Krasnikov, G. van den Bogaart, J. A. Killian, and B. Poolman, J. Am. Chem. Soc. **131**, 12650 (2009).
[12] T. H. Solomon, E. R. Weeks, and H. L. Swinney, Phys. Rev. Lett. **71**, 3975 (1993).
[13] F. Lechenault, R. Candelier, O. Dauchot, J. P. Bouchaud, and G. Biroli, Soft Matter **6**, 3059 (2010).
[14] S. Köhler, V. Schaller, and A. R. Bausch, Nat. Mater. **10**, 462 (2011).
[15] M. Chachisvilis, Y. Zhang, and J. A. Frangos, Proc. Natl. Acad. Sci. USA **103**, 15463 (2006).
[16] P. J. Butler, G. Norwich, S. Weinbaum, and S. Chien, Am. J. Physiol. Cell Physiol. **280**, C962 (2001).
[17] M. A. Haidekker, N. L'Heureux, and J. A. Frangos, Am. J. Physiol. Heart Circ. Physiol. **278**, H1401 (2000).
[18] R. Goetz and R. Lipowsky, J. Chem. Phys. **108**, 7397 (1998).
[19] A. Khoshnood, H. Noguchi, and G. Gompper, J. Chem. Phys. **132**, 025101 (2010).
[20] S. J. Marrink, H. J. Risselada, S. Yefimov, D. P. Tieleman, and A. H. de Vries, J. Phys. Chem. B **111**, 7812 (2007).
[21] M. P. Allen and D. J. Tildesley, *Computer Simulation of Liquids* (Oxford University Press, Oxford, 1991).
[22] H. S. Muddana, R. R. Gullapalli, E. Manias, and P. J. Butler, Phys. Chem. Chem. Phys. **13**, 1368 (2011).
[23] J. Neder, B. West, P. Nielaba, and F. Schmid, J. Chem. Phys. **132**, 115101 (2010).
[24] E. Flenner, J. Das, M. C. Rheinstadter, and I. Kosztin, Phys. Rev. E **79**, 011907 (2009).
[25] G. R. Kneller, K. Baczynski, and M. Pasenkiewicz-Gierula, J. Chem. Phys. **135**, 141105 (2011).
[26] M. J. Skaug, R. Faller, and M. L. Longo, J. Chem. Phys. **134**, 215101 (2011).
[27] M. Javanainen, H. Hammaren, L. Monticelli, J.-H. Jeon, M. S. Miettinen, H. Martinez-Seara, R. Metzler, and Ilpo Vattulainen, Faraday Discuss. **161**, 397 (2013).
[28] W. H. Press, S. A. Teukolsky, W. T. Vetterling, and B. P. Flannery, *Numerical Recipes: The Art of Scientific Computing*, 3rd ed. (Cambridge University Press, Cambridge, 2007).
[29] J. H. Argyris, G. Faust, and M. Haase, *An Exploration of Chaos: An Introduction for Natural Scientists and Engineers* (North-Holland, Amsterdam, 1994)
[30] J. M. Crane and A. S. Verkman, Biophys. J. **94**, 702 (2008).